A n-State Time-Domain Measurement Test-Bench for Characterization of Intermodulation Distortion on Device Level

Thomas Merkle, Suitbert Ramberger, Michael Kuri, Friedbert van Raay

Fraunhofer Institute for Applied Solid-State Physics (IAF), Tullastr. 72, D-79108 Freiburg, Germany

Abstract— **A flexible nonlinear measurement system is presented for the investigation of intermodulation distortion (IMD) on device level at Ka-band frequencies. The setup is unique in the way that a passive load-pull tuner embedded *inside* a full two-port test-set is combined with a hybrid receiver to one fully automated test system. The calibration problem of the resulting n-state test-set is formulated with a generalized 4-port error model, for the first time. The hybrid receiver is composed of a virtual 4 channel time-domain sampling oscilloscope and a spectrum analyzer. As an application, we show various two-tone sweep-scenarios applied to our GaAs HEMTs targeting high power applications at Ka-band frequencies.**

I. Introduction

SINCE the first introduction of load-pull measurement techniques to characterize transistors under various source and load match conditions [1], many different test-set configurations have been published. At the beginning, only passive load-pull tuners were used whereas later the active load-pull method [2] of the split signal path type and the feedback type became dominant. This is related to the emergence of full two-port test-sets for complete vectorial error correction. It renders the passive load match tuning outside the lossy input and output coupler pairs ineffective.

In the earlier days, frequency domain receiver concepts were used to access information about nonlinear effects in active devices. These receivers have still their right to exist for various single-tone load-pull tasks due to their speed and dynamic range [3]. Since the beginning of the 90s, however, modified time-domain sampling oscilloscopes (microwave transition analyzers, MTAs) have increasingly gained acceptance for accessing information about harmonic generation and time domain waveforms. It was mainly achieved due to the pioneering works in [4], [5], [6], [7], [8]. Drawbacks of the first generation MTAs are mainly their limited dynamic range for testing low spurious signals, their high data acquisition time, and the availability of only two synchronized channels. Thus, a hybrid receiver approach was proposed in [11] mainly inspired by the limited measurement speed of the two-channel MTA.

In this work, a different hybrid receiver approach composed of a first generation microwave transition analyzer and a spectrum analyzer is used to circumvent the problem of the limited dynamic range for spurious signal testing. Three advantages result from this approach: first reliability of measurement data acquired near noise level is assured. Second, below noise level, at least the accurate magnitude detection of the intermodulation products is possible. Third, instable operation modes on circuit level or device level can be discovered.

Works done at lower frequencies employed multi-tone signal sources to expand the active load-pull principle to intermodulation distortion measurements. In contrast, for two and three-tone measurements under various load conditions at millimeter wave frequencies, the passive load-pull principle is preferred in this work. However, the tuner is located inside the coupler pairs for the sake of higher impedance ratios. This has two reasons: First, although measurement equipment manufacturers made progress in expanding vector signal generation towards higher frequencies up to 20 GHz, a broadband tunable solution for all interesting Ka-band frequencies and above is still not available. Second, it is not practical with the active load-pull method of the split signal path type to realize circuit-like load terminations when modulation schemes of real communication systems are used.

In contrast to active load-pull setups, the passive load pull solution chosen in this work leads to the calibration of a full two-port n-state test-set. So far, to the authors knowledge, publications on calibration theory have mostly excluded this case.

II. Measurement Setup

In Fig. 1, the block diagram of our nonlinear measurement test-bench is depicted. Key feature of the system is its full two-port capability in conjunction with a two-channel microwave transition analyzer. This concept allows a vectorial correction

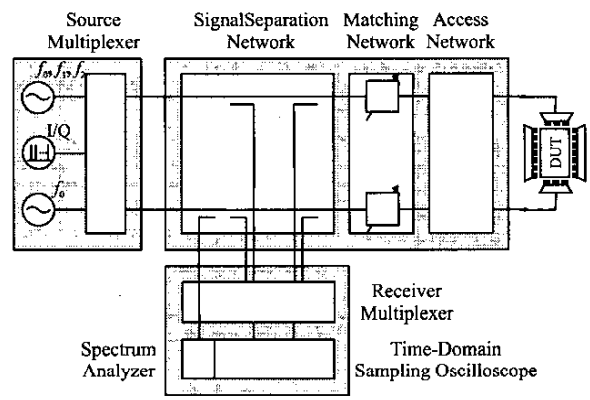

Fig. 1. Block diagram of the nonlinear measurement test-bench.

of all systematic measurement errors at the reference planes of the device under test (DUT). The two-channel transition analyzer is expanded to a *virtual* four-channel receiver by the receiver multiplexer composed of 2 transfer switches. This leads to a receiver with four different states. Each state corresponds to a different load and source termination for the DUT.

Under large-signal excitation of the DUT, however, one can not judge from a measurement made for one termination of the DUT about a measurement made for another termination of the DUT. Thus, either the impacts of the different receiver states on the signal separation network have to be minimized

0-7803-7695-1/03/$17.00 © 2003 IEEE

by attenuators and high coupling factors, or the receiver multiplexer has to be made absorbing under any switching state. The latter measure was applied to reduce the 4-state receiver to a 1-state receiver as close as possible. Additionally, for low spurious signal testing the attenuation was chosen just large enough to make sure that the receiver is not overdriven and generates spurious signals by itself.

Virtual four-channel receivers can not simultaneously measure all 4 power waves. This means for harmonic testing that absolute measurements of the power waves have to be taken to establish the phase relation between harmonics and fundamentals and additional relative measurements are necessary to establish the phase relations between the 4 power waves.

The dynamic range of transition analyzers is restricted and further deteriorating towards higher frequencies. This is eliminated for spurious signal testing by adding a conventional spectrum analyzer at the output of the test-set. Fig. 2 shows upper and lower third order intermodulation distortion (IMD3L/H) measurements of a GaAs single-recess pHEMT transistor obtained by the transition analyzer and the spectrum analyzer. The measurements of the IMD3 close to noise level

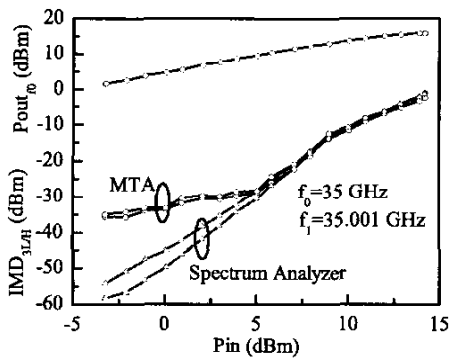

Fig. 2. Hybrid receiver approach: two-tone intermodulation (IM) measurements of a 8x60 μm wide single-recess GaAs pHEMT transistor measured on 50 Ω at 35 GHz (IAF technology). Gate length 0.15 μm. Biasing scheme class A.

using the transition analyzer can be misinterpreted without the information of the spectrum analyzer. This is especially disturbing when nulling effects in the intermodulation behavior are concealed by noise. In Fig. 3, measurements of a device with same lateral layout as the device shown in Fig. 2 but with a double-recess gate module are depicted. Here nulling effects can be observed which depend on biasing conditions.

It has to be mentioned at this point that the bandwidth of usual signal separation networks composed of directional couplers does not cover measurements of baseband intermodulation components. However, according to [9] the influence of these components on third order intermodulation products should be considered. Thus, in [10] a low frequency signal separation network realized in the biasing networks was proposed. In our work only the baseband components' termination is determined a-priori with a low frequency network analyzer (NWA).

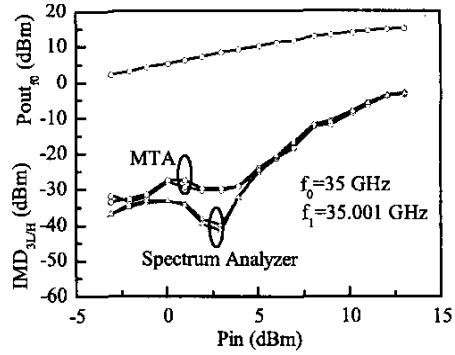

Fig. 3. Intermodulation behavior of a 8x60 μm wide double-recess pHEMT transistor on 50 Ω at 35 GHz. Gate length 0.15 μm. Biasing scheme class A.

Two strategies to generate test signals are followed: additive generation of two-tone and three-tone signals and baseband generation of digital modulated signals. For the first strategy the nonlinear measurement test-bench is equipped with three single-tone signal sources. They can be combined in any way to either additively generate two-tone and three-tone signals or to simultaneously excite input and output of the DUT for harmonic active load-pull or injection of spurious fundamental signals at the output. For the second approach, the use of baseband arbitrary waveform generators is pursued in this work. This method is extended towards frequencies at the Ka-band with a two step up-conversion.

III. System Calibration

The implemented generalized 4-port error model is shown in Fig. 4. Starting from the relative [12] and absolute [7] 4-port 1-state error model, the general n-state test-set case can

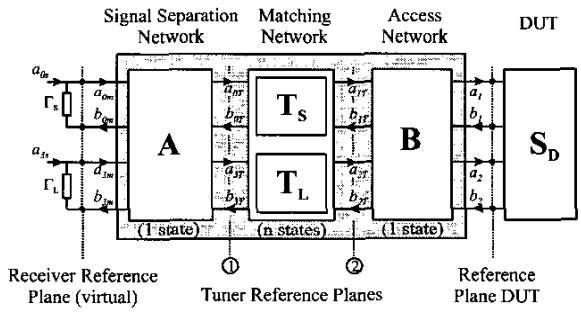

Fig. 4. Implemented generalized n-state 4-port error model.

be described by

$$\begin{bmatrix} a_{0m} \\ b_{0m} \\ \hline a_{3m} \\ b_{3m} \end{bmatrix} = \alpha \cdot \left[\begin{array}{c|c} \mathbf{T_{11}} & \mathbf{T_{12}} \\ \hline \mathbf{T_{21}} & \mathbf{T_{22}} \end{array}\right]_{(n)} \begin{bmatrix} a_1 \\ b_1 \\ \hline a_2 \\ b_2 \end{bmatrix}$$

$$= \alpha \cdot \mathbf{T_{e,(n)}} \begin{bmatrix} a_1 \\ b_1 \\ \hline a_2 \\ b_2 \end{bmatrix} \quad (1)$$

were α is the absolute calibration coefficient and $\mathbf{T_{ij}}$ are two-port block matrices. Eq. (1) can be separated according to the block diagram in Fig. 4 into a signal separation error model and an access error model which both do not change for different matching conditions. This means for $\mathbf{T_{e,(n)}}$ that

$$\mathbf{T_{e,(n)}} = \underbrace{\left[\begin{array}{c|c} \mathbf{A_{11}} & \mathbf{A_{12}} \\ \hline \mathbf{A_{21}} & \mathbf{A_{22}} \end{array}\right]}_{1-state} \underbrace{\left[\begin{array}{c|c} \mathbf{T_{11}} & \mathbf{T_{12}} \\ \hline \mathbf{T_{21}} & \mathbf{T_{22}} \end{array}\right]}_{n-state} \underbrace{\left[\begin{array}{c|c} \mathbf{B_{11}} & \mathbf{B_{12}} \\ \hline \mathbf{B_{21}} & \mathbf{B_{22}} \end{array}\right]}_{1-state}$$

$$= \mathbf{A_{(1)}} \mathbf{T_{(n)}} \mathbf{B_{(1)}} \quad (2)$$

The signal separation model represents the input and output directional couplers plus possible crosstalk at source switches. The error box of the access network models the on-wafer probe tips plus possible crosstalk and the access lines (either waveguide or coaxial) to the output reference plane of the mechanical tuners. It is reasonable to assume that no crosstalk appears at the matching network when it is composed of mechanical waveguide or coaxial tuners and

$$\mathbf{T_{12}} = \mathbf{T_{21}} = \mathbf{0} \quad (3)$$

The relative calibration according to Eq. (1) needs minimum $n \cdot k_{min}$ measurements where n is the number of different matching conditions and k_{min} is the minimum number of calibration standards to be measured for each state. For example, the self calibration procedures of the 8-term error model require a minimum of k_{min} = 3 full two-port standards to be measured [13]. Besides the large number of necessary measurements for calibration another drawback of this approach results from the nature of mechanical tuners: they show high losses when very high reflection coefficients have to be realized. The losses of a mechanical sliding screw tuner in dependence of the stepper motor positions are depicted in Fig. 5 for a tuner load plane at 35 GHz. With more than 10 dB loss for high reflection coefficients, the directivity of the test-set is deteriorated to an unacceptable level at Ka-band frequencies, especially critical in conjunction with the low dynamic range of first generation microwave transition analyzers.

In contrast to the paragraph above, in this work reference planes ① and ② were established to separate Eq. (2) into parts independent and dependent from matching conditions. The tuner itself was calibrated a-priori with a conventional network analyzer for reasons of speed and accuracy. The reproducibility of the mechanical tuners was confirmed to be in the range of calibration to calibration variations. Fig. 6 shows the remaining transmission errors for a thru standard measurement within the load plane at 20 GHz. This procedure allowed to reduce the necessary number of calibration steps considerably.

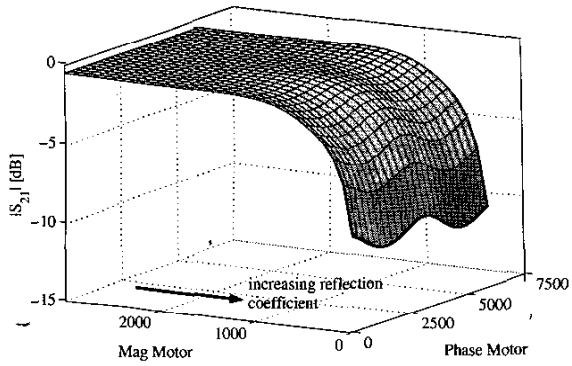

Fig. 5. Losses of a mechanical sliding screw tuner at a load plane of 35 GHz. The x-axis and y-axis are the positions of the stepper motors to adjust the load match conditions.

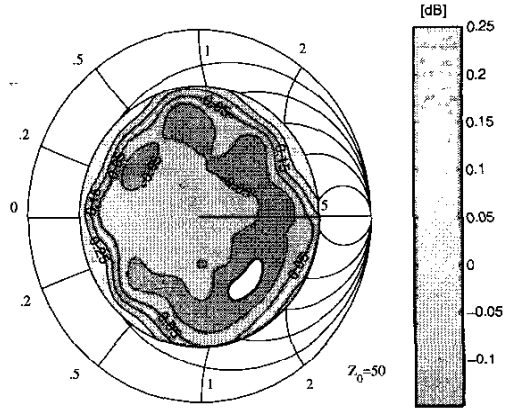

Fig. 6. Verification measurements with a thru for different load conditions. Depicted is the measured transmission coefficient in dB for the separation approach according to Eq. (2) at 20 GHz.

IV. Application Examples

The optimization of the intermodulation ratio (IMR) on device level requires the search in a multidimensional parameter space. Thus, we have spent a considerable effort in developing our own in-house software which is capable of performing this task in a fully automated way. This is especially important for all statistical analysis of, for example wafer homogeneity and batch to batch variations. Fig. 7 and Fig. 8 show load-pull measurements under single-tone and two-tone excitation performed on a single-recess GaAs pHEMT structure. For both measurements we selected 63 different load conditions at the DUT reference plane on an equidistant grid indicated by the dots in Fig. 7. For potentially instable devices, instability regions can be excluded from the list of load conditions to be measured. In Fig. 9 the IMR for a double-recess transistor was measured at a fixed input power level for all interesting bias conditions. For this device, it can be observed that biasing closer to pinch-off at V_{gs} = -0.5 V leads to an improved IM performance compared to biasing at maximum transconductance at V_{gs} = -0.3 V. This biasing guideline was also observed on our single-recess technology, on device level as well as on circuit level [14].

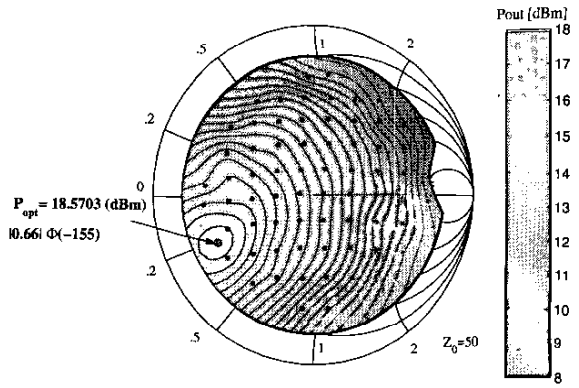

Fig. 7. One-tone load-pull measurement of our single-recess GaAs pHEMT transistor (IAF technology) at 35 GHz. The total gatewidth is 0.48 μm. The input power was held constant at 10 dBm.

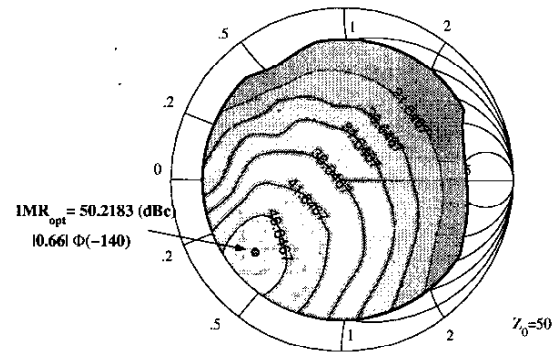

Fig. 8. Intermodulation ratio (IMR) contours for the same device as in Fig. 7 at 35 GHz. Tone spacing is 1 MHz. The output power was held constant at 10 dBm per tone.

V. Conclusions

A flexible measurement test-bench for characterization of intermodulation distortion at Ka-Band frequencies under realistic load conditions was presented. In contrast to previous works on time-domain waveform measurement systems, a *passive* load-pull tuner was used *inside* the full two-port test-set. The calibration of the resulting n-state test-set was treated in the most general way of 4-port error networks. The resulting errors are sufficiently small for reflection factors up to a magnitude $|\Gamma| = 0.7$ and frequencies up to the Ka-band. To handle the multidimensional minimization problem of intermodulation distortion on device level, a extensive in-house software was developed which is based on the generalized n-state 4-port error model.

VI. Acknowledgments

The authors would like to thank M. Schlechtweg and G. Weimann for their ongoing support of this work. This work was funded by the German Ministry of Education and Research (BMBF).

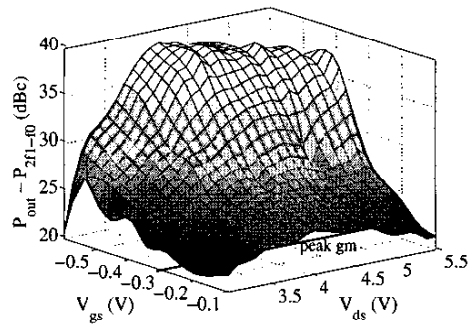

Fig. 9. IMR under different bias conditions for a double-recess HEMT transistor at 35 GHz. Input power is 8 dBm per tone. 1 MHz tone spacing.

References

[1] J. M. Cusack, S. Perlow, B. Perlman, "Automatic load contour mapping for microwave power transistors", *IEEE Transactions on Microwave Theory and Techniques*, vol. 22, no. 12, pp. 1146-1152, Dec. 1974.

[2] Y. Takayama, "A new load-pull characterization method for microwave power transistors", *IEEE MTT-S International Microwave Symposium Digest*, pp. 218-220, 1976.

[3] B. Hughes, A. Ferrero, A. Cognata, "Accurate on-wafer power and harmonic measurement of mm-wave amplifiers and devices", *IEEE MTT-S International Microwave Symposium Digest*, pp. 1019-22, 1992.

[4] M. Sipilä, K. Lehtinen, V. Porra, "High-frequency periodic time domain waveform measurement system", *IEEE Transactions on Microwave Theory and Techniques*, vol. 36, no. 10, pp. 1397 1405, Oct. 1988.

[5] F. Van Raay, G. Kompa, "A new on-wafer large-signal waveform measurement system with 40 GHz harmonic bandwidth", *IEEE MTT-S International Microwave Symposium Digest*, pp. 1435-1438, 1992.

[6] M. Demmler, P. J. Tasker, M. Schlechtweg, "A vector corrected high power on-wafer measurement system with a frequency range for the higher harmonics up to 40 GHz", *24th European Microwave Conference*, pp. 1367-1372, 1994.

[7] T. Van den Broeck, J. Verspecht, "Calibrated vectorial nonlinear-network analyzers", *IEEE MTT-S International Microwave Symposium Digest*, pp. 1069-1072, 1994.

[8] J. Verspecht, P. Debie, A. Barel, L. Martens, "Accurate on wafer measurement of phase and amplitude of the spectral components of incident and scattered voltage waves at the signal ports of a nonlinear microwave device", *IEEE MTT-S International Microwave Symposium Digest*, pp. 1029-1032, 1995.

[9] J. F. Sevic, K. L. Burger, M. B. Steer, "A novel envelope-termination load-pull method for ACPR optimization of RF/microwave power amplifiers", *IEEE MTT-S International Microwave Symposium Digest*, pp. 723-726, 1998.

[10] D. J. Williams, J. Leckey, P. J. Tasker, "A study of the effect of envelope impedance on intermodulation asymmetry using a two-tone time domain measurement system", *IEEE MTT-S International Microwave Symposium Digest*, pp. 1841-1844, 2002.

[11] A. Ferrero, V. Teppati, "A complete measurement test-set for non-linear device characterization.", *58th ARFTG Automatic RF Techniques Group Conference*, CDROM digest pp. 133-135, 2001.

[12] J. V. Butler, D. K. Rytting, M. F. Iskander, R. D. Pollard, M. Vanden Bossche, "16-term error model and calibration procedure for on-wafer network analysis measurements.", *IEEE Transactions on Microwave Theory and Techniques*, vol. 39, no. 12, pp. 2211-2217, Dec. 1991.

[13] H. J. Eul, B. Schiek, "A generalized theory and new calibration procedures for network analyzer self-calibration.", *IEEE Transactions on Microwave Theory and Techniques*, vol. 39, no. 4, pp. 724-731, Dec. 1991.

[14] T. Merkle, A. Tessmann, S. Ramberger, "Intercept point behavior of Ka-band GaAs high power amplifiers.", *IEEE MTT-S International Microwave Symposium Digest*, pp. 453-456, 2001.